

## LETTERS

### Direct Synthesis of High Purity Single-Walled Carbon Nanotube Fibers by Arc Discharge

Huanjun Li, Lunhui Guan, Zujin Shi, and Zhennan Gu\*

*Department of Chemistry, Peking University, Beijing 100871, P.R. China*

*Received: August 28, 2003; In Final Form: February 4, 2004*

Long fibers of high purity single-walled carbon nanotubes (SWNTs) were directly synthesized macroscopically by the modified arc discharge method. The purity of SWNT in fibers that can be obtained, as high as 80% (volume), was evaluated by scanning electron microscopy, thermogravimetric analysis, and Raman spectroscopy. The diameters of the SWNT fibers we obtained vary from 2 to 200  $\mu\text{m}$  with a predomination of 5–20  $\mu\text{m}$ . The lengths can reach as long as 10 centimeters. It is proposed that promoter FeS is a crucial factor for synthesizing high purity SWNT fibers.

Since their discovery in 1993,<sup>1</sup> single-walled carbon nanotubes (SWNTs) have attracted extensive interest of scientists all over the world, for they offer the prospect of both new fundamental science and useful technological application.<sup>2–5</sup> Unfortunately, as-grown SWNTs contain a great amount of impurities such as metal catalyst, carbon nanoparticles, and amorphous carbon. Purifying SWNTs is tedious and time-consuming work. Furthermore, commonly used purifying processes including thermal oxidation in air and acid refluxing, unavoidably bring defects to SWNTs themselves. These hamper their applications in mechanical and electrical fields. A prerequisite step for the industrial applications of SWNTs is to obtain well-aligned, high purity, and low defect SWNTs that allow facile measurement of the various physical and chemical properties.

In 1998, Cheng et al. synthesized long and wide ropes of SWNT bundles by the catalytic decomposition of hydrocarbons.<sup>6</sup> Before long, macroscopic SWNT fibers and ribbons made by postprocessing techniques were already been reported.<sup>7</sup> Recently Cheng et al.<sup>8</sup> and Wu et al.<sup>9</sup> synthesized orderly SWNT strands by  $\text{H}_2$ –Ar arc discharge and the floating chemical vapor deposition (CVD) method, respectively. In contrast to the CVD method, SWNTs synthesized by arc discharge show more superiority, for they have higher crystallinity, such as their higher

crystallinity. In this work, we modified the arc discharge conditions and achieved high purity (80% in volume) SWNT fibers. The diameters of the SWNT fibers we obtained vary from 2 to 200  $\mu\text{m}$  with a predomination of 5–20  $\mu\text{m}$ , and the lengths can reach as long as 10 cm.

In our experiments, SWNT fibers were produced by the dc arc discharge method similarly to that reported in our earlier work.<sup>10,11</sup> The cathode was a  $8 \times 200$  o.d. mm graphite rod with a sharp end toward the anode. A  $4 \times 100$  o.d. mm hole was drilled in a  $6 \times 150$  o.d. mm spectrally pure graphite rod and filled with graphite powder, Y–Ni alloy ( $\text{YNi}_2$ ), and a small quantity of FeS with weight ratio of 80:20:1.5. The arc discharge was created by a current of 80 A in a helium atmosphere at a pressure of 760 Torr. The arc was maintained by continuously translating the cathode to keep a constant distance ( $\sim 3$  mm) between it and the anode. Typical synthesis time was 15 min. The SWNT fibers were obtained on the top of the cathode. The as-prepared SWNT fibers were characterized by scanning electron microscope (SEM, JEOL, JSM-6700F), thermogravimetric analysis (TGA Dupont Instrument, 951 TGA), Raman spectroscopy (Renishaw system 2000 UK), and X-ray diffraction measurements (XRD, Rigaku Duax/2000).

SWNT fibers were collected from the top area of the cathode. They are free-standing and strongly adhering to the cathode and have a length of several centimeters. Besides the fibers, cotton-like and cloth-like raw soot can also be obtained from the inner

\* Corresponding author. E-mail: guzn@chem.pku.edu.cn.

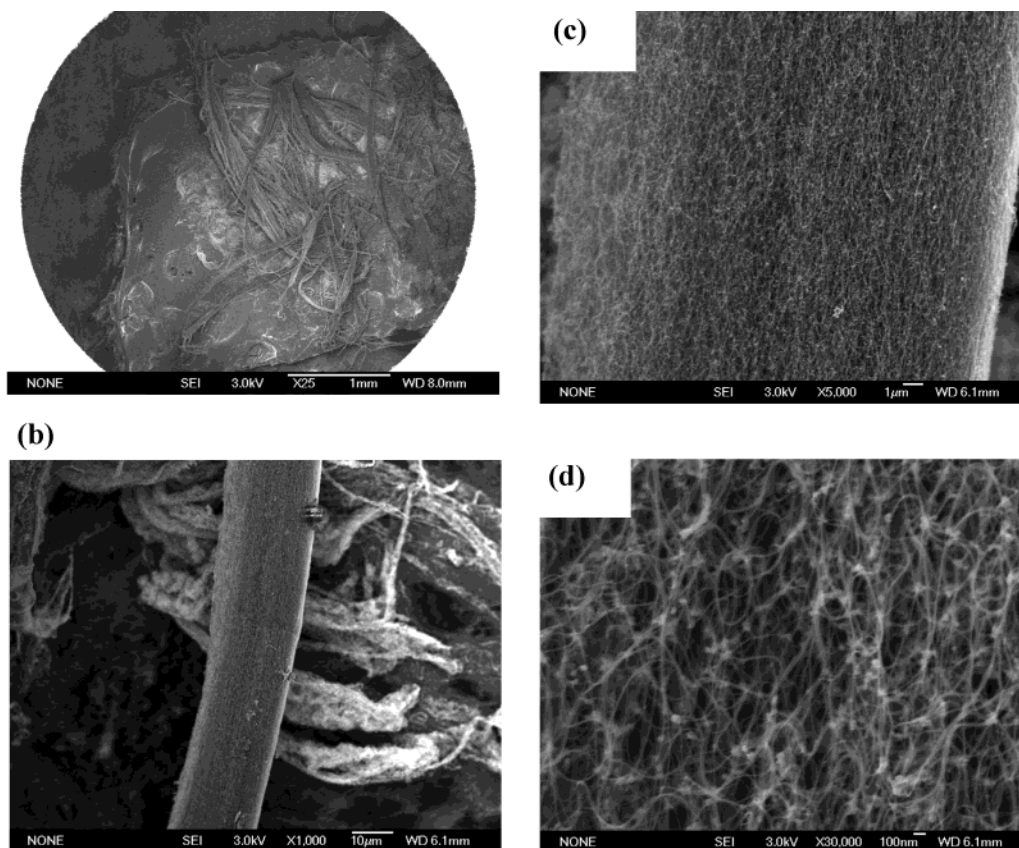


**Figure 1.** (a) SEM image of as-prepared fibrous materials composed of many SWNTs fibers, (b) SEM image of a typical SWNTs fiber at  $1\times$  magnification, (c) SEM image of the typical SWNTs fiber at  $5\times$  magnification, and (d) SEM image of the typical SWNTs fiber at  $30\times$  magnification.

wall of the chamber. For SEM measurement, fibers were cut and fixed on the sample stage. Figure 1a shows a low magnification SEM image of SWNT fibers. From the figure, it can be seen that most of the SWNT fibers are as long as several millimeters. In view of the bending of the SWNT fibers and the limit of visual field, their actual lengths can extend to several centimeters. The diameters of SWNT fibers spread within a range from 2 to  $200\ \mu\text{m}$  with the predominant value from 2 to  $5\ \mu\text{m}$ . From the figure of a typical SWNT fiber with a diameter of  $20\ \mu\text{m}$  (Figure 1b), we can find that the edges of SWNT fiber are smooth and continuous, with a few SWNT bundles sticking out of the edge.

Parts c and d of Figure 1 show a higher magnification of this typical  $20\ \mu\text{m}$  diameter SWNT fiber. A high purity and well-aligned SWNT fiber can be found in this figure. The fiber is composed of abundant snarled SWNT bundles. Only a few impurities can be found sticking to the SWNT bundles. From the figure, the purity (volume) is estimated to be as high as over 80%.

To investigate the weight purity of SWNT in the fibers, we performed thermogravimetric analysis (TGA). Precise estimation of the purity of SWNTs is very difficult, but it is easy to measure the catalyst content in our products by means of TGA. Figure 2 shows the TGA graph of the SWNT fibers; the SWNTs are completely burned out near  $900\ ^\circ\text{C}$ . The remaining material is the transition metal oxide, which is about 38 wt %. From the figure, it is estimated that Ni accounts for nearly 30 wt % in our raw products. As to the different density between Ni and SWNT, the volume ratio of metal in the raw products is below 20%.

The Raman scattering technique has also been used to characterize the purity and to determine the diameter of SWNTs.<sup>12</sup> The diameter of individual SWNT can be determined

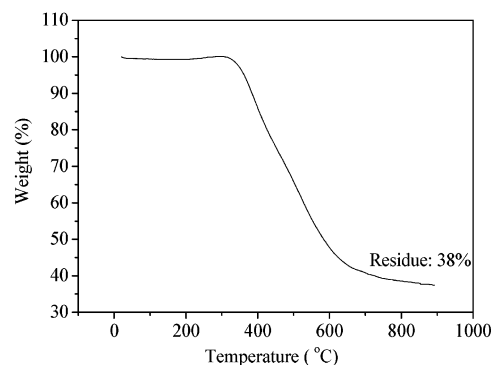


**Figure 2.** TGA curves of the SWNT fibers.

by the radial breathing mode (RBM) from 100 to  $300\ \text{cm}^{-1}$ . The Raman spectrum was collected using a  $514.5\ \text{nm}$  line of an  $\text{Ar}^+$  laser for excitation and a  $50\times$  objective at room temperature and ambient pressure. The SWNT fibers were adhered to a glass surface. The Raman spectra taken from different areas along the fibers are similar to each other, showing homogeneity along the strands. Typical Raman spectra of as grown SWNT fibers and cloth-like SWNTs are shown in Figure 3. The sharp G-band modes that can be clearly seen in the spectrum indicate a good arrangement of the hexagonal lattice of graphite. The distinctive peak at  $1562\ \text{cm}^{-1}$  on the left shoulder of the main G band and a low intensity of the D-band (intensity of G/D = 30.2) indicate high purity of as-grow SWNT fibers.<sup>13,14</sup> According to the following correlation<sup>15</sup> between diameter  $d$  (nm) and frequency  $\omega$  ( $\text{cm}^{-1}$ ),  $d = 224/(\omega - 14)$ , nanotubes with predominantly  $1.28\ \text{nm}$  (peak centered at  $188\ \text{cm}^{-1}$ ) and  $1.49\ \text{nm}$  (peak centered at  $164\ \text{cm}^{-1}$ ) diameters are present in the SWNT fibers and cloth-like raw soot, respectively. It is a highly debated issue why the diameter of SWNT in fibers

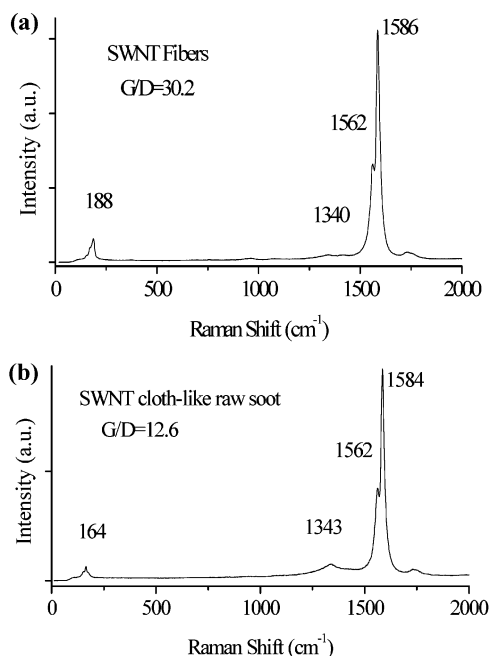


**Figure 3.** Raman spectra of (a) SWNT fibers and (b) SWNTs cloth-like raw soot.

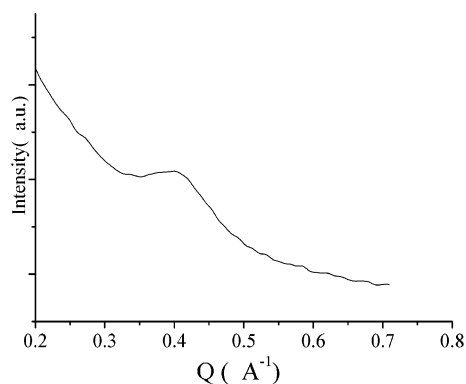


**Figure 4.** Typical X-ray diffraction pattern from SWNT fibers.

is less than that in cloth-like raw soot. The temperature gradient is a potential cause of this phenomenon. In our arc experiments, the wool-like root can be seen ejecting from the center of the arc and then adhering to the chamber wall to form the cloth-like raw soot, whereas the SWNT fibers are found in the localized region around the cathode. It is commonly accepted that in the dc arc discharge, one of the key factors is the temperature gradient. In the center of the arc, a high temperature regime (above 4000 °C) is responsible for the synthesis of the cloth-like raw soot. On the cathode, however, we assume that the temperature is reduced rapidly thanks to the water cooling. Thus, we estimated that the favorable temperature of formation of SWNT fibers ranges from 1000 to 2000 °C. As to the cloth-like raw soot, the corresponding temperature is above 4000 °C.

We performed XRD at room temperature with the Cu K $\alpha$  ( $\lambda = 1.542$  Å) line in the X-ray diffractometer operated at 50 kV and 120 mA. The SWNT fibers were adhered parallel with the 2.5 cm side in the sample holder that has a rectangular hole with a size of 1.5 cm  $\times$  2.5 cm. The low- $Q$  (scattering vector  $Q = 4\pi \sin \theta/\lambda$ ) region is dominated by small angle scattering. In Figure 4, a broad peak centered at  $Q = 0.4$  Å $^{-1}$  ( $2\theta \sim 6^\circ$ ) corresponds to  $d(1, 0)$  of a two-dimensional (2D) hexagonal

lattice. The corresponding lattice parameter calculated from this peak is 1.7 nm, which is quite accorded with the lattice parameter<sup>16</sup> of an ideal lattice assembled from 1.3 nm diameter nanotubes. The XRD result confirms the results from Raman measurements that 1.3 nm tubes dominate the fibers.

In the synthesis of SWNT fibers, we found that choosing FeS as promoter was critical. Transition metals have widely been used to produce SWNTs by arc discharge. However, SWNT fibers have rarely been reported by arc discharge using Y–Ni alloy as catalyst. In our study, without FeS, the quality and quantity of SWNT fibers decrease rapidly. From recent reports about the synthesis of SWNT strands or superbundles by H $_2$ –Ar arc discharge<sup>8</sup> and floating CVD,<sup>9</sup> a little sulfur-containing compound as promoter is necessary. It has been reported that<sup>17</sup> the presence of a spot of S assists the graphitization of the nanotube on the cathode and promotes the catalytic action of the metal by giving a more favorable crystallographic orientation for the catalytic adsorption. This helps the growth of SWNT fibers in a given orientation.

In short, well-aligned long SWNT fibers, consisting of numerous SWNT bundles, were macroscopically synthesized by the modified arc discharge method under the existence of YNi $_2$  catalyst and small amount of FeS promoter. These long fibers with high crystallinity will be convenient to handle and manipulate, suggesting a broad use as electrical connects, or as building blocks.

**Acknowledgment.** This work is supported by the National Natural Science Foundation of China under Grant Nos. 20151002 and 90206048, the Doctoral Program Foundation of the Ministry of Education of China and the Postdoctoral Science Foundation of China.

## References and Notes

- (1) Iijima, S.; Ichihashi, T. *Nature* **1993**, 363, 603.
- (2) Treacy, M. M. J.; Ebbesen, T. W.; Gibson J. M. *Nature* **1996**, 381, 678.
- (3) Avouris, P. *Acc. Chem. Res.* **2002**, 35, 1026.
- (4) . Dillon, A. C.; Jones, K. M.; Bekkedahl, T. A.; Kiang, C. H.; Bethune, D. S.; Heben, M. J. *Nature* **1997**, 386, 377.
- (5) Baughman, R. H.; Zakhidov, A. A.; de Heer W. A. *Science* **2002**, 397, 787.
- (6) Cheng, H. M.; Li, F.; Sun, X.; Brown, S. D. M.; Pimenta, M. A.; Marucci, A.; Dresselhaus, D.; Dresselhaus, M. S. *Chem. Phys. Lett.* **1998**, 289, 602.
- (7) Vigolo, B.; Penicaud, A.; Coulon, C.; Sauder, C.; Pailler, R.; Journet, C.; Bernier, P.; Poulin, P. *Science* **2000**, 290, 1331.
- (8) Liu, C.; Cheng, H. M.; Cong, H. T.; Li, F.; Su, G.; Zhou, B. L.; Dresselhaus, M. S. *Adv. Mater.* **2000**, 12, 1190.
- (9) Zhu, H. W.; Xu, C. L.; Wu, D. H.; Wei, B. Q.; Vajtai, R.; Ajayan, P. M. *Science* **2002**, 296, 884.
- (10) Shi, Z. J.; Lian, Y. F.; Zhou, X. H.; Gu, Z. N.; Zhang, Y. G.; Iijima, S.; Li, H. D.; Yue, K. T.; Zhang, S. L. *J. Phys. Chem. B* **1999**, 103, 8698.
- (11) Shi, Z. J.; Lian, Y. F.; Zhou, X. H.; Gu, Z. N.; Zhang, Y. G.; Iijima, S.; Zhou, L. X.; Yue, K. T.; Zhang, S. L. *Carbon* **1999**, 37, 1449.
- (12) Kasuya, A.; Sasaki, Y.; Saito, Y.; Tohji, K.; Nishina, Y. *Phys. Rev. Lett.* **1997**, 78, 4434.
- (13) Duesberg, G. S.; Loa, I.; Burghard, M.; Syassen, K.; Roth, S. *Phys. Rev. Lett.* **2000**, 85, 5436.
- (14) Kataura, H.; Kumazawa, Y.; Maniwa, Y.; Ohtsuka, Y.; Sen, R.; Suzuki, S.; Achiba, Y. *Carbon* **2000**, 38, 1691.
- (15) Rao, A. M.; Chen J.; Richter E.; Schlecht U.; Eklund P. C.; Haddon, R. C.; Venkateswaran, U. D.; Kwon, Y. K.; Tom anek D. *Phys. Rev. Lett.* **2001**, 86, 3895.
- (16) Thess A.; Lee R.; Nikolaev P.; Dai, H. J.; Petit, P.; Robert, J.; Xu, C. H.; Lee, Y. H.; Kim, S. G.; Rinzler, A. G.; Colbert, D. T.; Scuseria, G. E.; Tomanek, D.; Fischer, J. E.; Smalley, R. E. *Science* **1996**, 273, 483.
- (17) Demoncey, N.; Stéphan, O.; Brun, N.; Colliex, C.; Loiseau, A.; Pascard, H. *Eur. Phys. J. B* **1998**, 4, 147–157.